

## Supporting information for:

### In Situ Electrical Modulation and Monitoring of Nanoporous Gold Morphology

Tatiana Dorofeeva, Erkin Seker\*

Department of Electrical and Computer Engineering, University of California – Davis, Davis, CA

\*Corresponding author: [eseker@ucdavis.edu](mailto:eseker@ucdavis.edu)

#### Closed-Loop Electro-Annealing

Electro-annealing setup from our earlier work was modified to include closed-loop temperature control.<sup>1</sup> Briefly, basic electro-annealing fixture consists of polychlorinated biphenyl (PCB) board and glass slide with aluminum foil sandwiched between the two (for improved temperature distribution). The np-Au sample is placed on top of the glass slide and secured via two conductive screw-tightened clips. Current is injected into np-Au through the clips via the power supply. Temperature of the np-Au is measured using IR thermometer which is secured above the sample. Emissivity setting of the infra-red (IR) thermometer was set to 0.17 (for more discussion how this value was selected see Supporting Information in previous work).<sup>1</sup> Several modifications were subsequently made to the setup to improve the measurement accuracy and to enable full automation of the annealing process (Figure S1A).

The electrical current was obtained directly from the power supply; however, voltage measurements from the power supply lacked sufficient accuracy. To overcome this, we used a digital oscilloscope (Analog Discovery by Digilent) to obtain voltage drop across the sample. All three measurement devices (i.e., power supply, digital oscilloscope, and thermometer) were connected to a computer via USB cables. A custom MatLab software was created to improve ease of user interface with the equipment and to develop custom annealing protocols. Closed-loop annealing was implemented through PID controls. A typical closed-loop control starts by setting a starting current value (usually low enough that temperature remains close to room temperature). Temperature measurements is then taken after several seconds of applying current. The error value between set and measured temperatures is calculated and used to estimate a new current value. This step sequence is continuously cycled until the test time has elapsed. The PID values were adjusted to obtain an optimal compromise between fast ramping (<60 s) while at the same time minimizing temperature overshoot to less than 10°C. Measured current, voltage, and temperature values were continuously updated and displayed on the screen in a graphical format. An example printout of the data obtained during constant temperature annealing test is shown in Figure S1B. Electrical connection schematic is shown in Figure S1C.

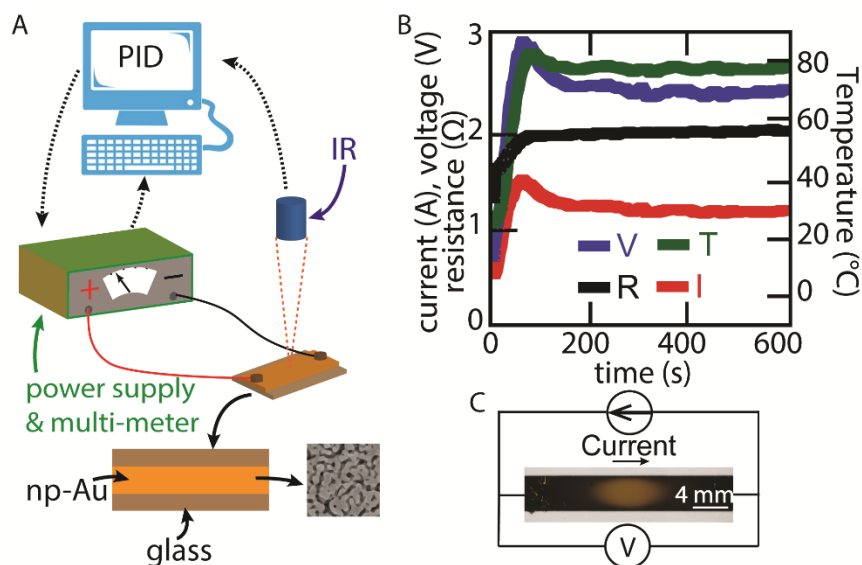


**Figure S1.** A) Illustration of the experimental setup. B) A representative measurement data output. C) Schematic illustrating the electrical connections.

### Electrical Resistance Calculations

The resistance of each sample was computed assuming each ligament is a wire that extends an entire length of the sample. Total resistance is assumed to be a large number of nanowires in parallel. Resistance of each sample was computed using:

$$R = \frac{\rho * l}{\frac{w}{d} \cdot \frac{t}{d} \cdot A}$$

Where  $l$  is distance between clips used to make contact to the sample (17 mm) and also length of each wire,  $w$  is sample width (2 mm) and  $t$  is sample thickness (see values in Table S1),  $d$  is ligament thickness,  $w/d$  and  $t/d$  is number of wires that can fit in cross-sectional area of the sample, and  $A$  is a cross sectional area of a single ligament  $A = \pi * (d/2)^2$  and  $\rho$  is resistivity of a single ligament.

For each sample, image analysis was performed to extract ligament thickness from top-view SEM images. The film thickness was measured directly for the control, 60, 70 and 90°C annealing temperatures using cross-sectional SEM images. Five thickness measurements for each temperature case were averaged. These values were used to estimate the remaining film thicknesses by fitting second order polynomial to measured data and extrapolating the remaining data points (Figure S2A). Defect spacing (grain size) was measured manually for highly annealed samples (70, 80, and 90°C), 20 measurements per sample were averaged to obtain the mean defect spacing. For the as-dealloyed and slightly annealed samples (ctrl, 50 and 60°C), defect spacing was back-calculated to match measured dR% values. The reason behind this is that in these samples ligaments are too small to discern defects directly from SEM images. Calculated defect spacing fit well with the prediction that as-dealloyed material contains very few defects,<sup>2</sup> but defect spacing increases with annealing. Superimposing estimated and

measured defect spacing revealed good fit at the high annealing temperatures range as shown in Figure S2B.

**Table S1.** Ligament size, film thickness and defect spacing values extracted for each annealing temperature. \* Values were extrapolated by curve-fit analysis based on values measured. #Values were calculated based on measured dR% values.

Sample Name	Annealing Temperature (°C)	Median Ligament Size (nm)	Film Thickness (nm)	Defect spacing (nm)
ctrl	27	56	542	500 <sup>#</sup>
50°C	50	56	520*	150 <sup>#</sup>
60°C	60	76	507	60 <sup>#</sup>
70°C	70	112	490*	41
80°C	80	156	473	32
90°C	90	165	450	23

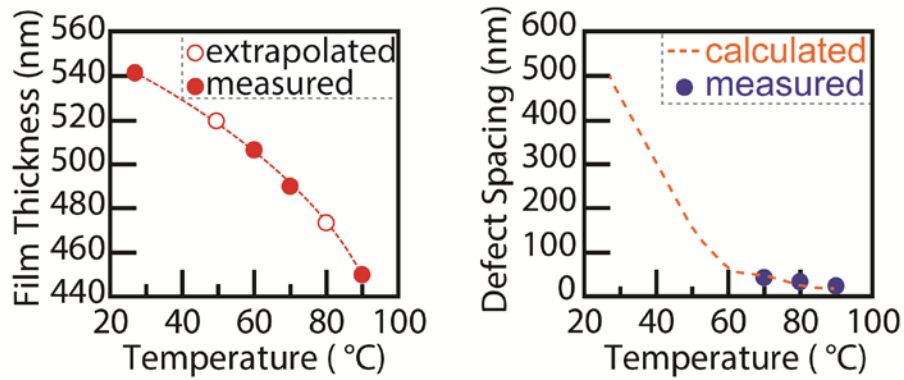


**Figure S2.** A) Film thickness and B) defect spacing (average grain size) measurement and estimation

Resistivity of a single ligament was obtained from Wiedemann-Franz law:

$$\rho = \frac{1}{\sigma} = \frac{L \cdot T}{\lambda_s}$$

Where  $L$  is Lorentz number,  $T$  is the temperature (in this case 300K) and  $\lambda_s$  is thermal conductivity of a single ligament. Thermal conductivity for a single ligament was computed using:<sup>3</sup>

$$\lambda_s = \frac{1}{3} v_F^2 \frac{\gamma T}{AT^2 + BT + v_F/d_{an} + v_F/l_{an}^*}$$

Where  $v_F$  is Fermi velocity,  $d_{an}$  is median ligament thickness,  $AT^2$  is reciprocal of the electron-electron scattering time,  $BT$  is reciprocal of electron-phonon scattering time,  $v_F/d_{an}$  is reciprocal of electron-surface scattering time, and  $v_F/l_{an}^*$  is the reciprocal of the electron-defect scattering. Also,  $l_{an}^* = l_{an}(1-\Gamma)/\Gamma$  where  $l_{an}$  is mean defect spacing and  $\Gamma$  is electron reflection coefficient. Table 2 summarizes the values that were used for calculation.<sup>3</sup>

**Table S2.** Symbols and values used for calculating thermal resistivity of a single ligament

Symbol	Value
$v_F$	1.6e6 m/s
$\gamma$	62.7 J m <sup>-3</sup> K <sup>-2</sup>
$A$	1.2e7 K <sup>-2</sup> s <sup>-1</sup>
$B$	1.23e11 K <sup>-1</sup> s <sup>-1</sup>
$T$	300 K
$\Gamma$	0.3
$L$	2.45e-8 W $\Omega$ K <sup>-2</sup>

Figure S3A demonstrates the impact of varying defect spacing on the overall resistance of each sample. The impact of varying ligament thickness while keeping defect spacing as measured is also shown.

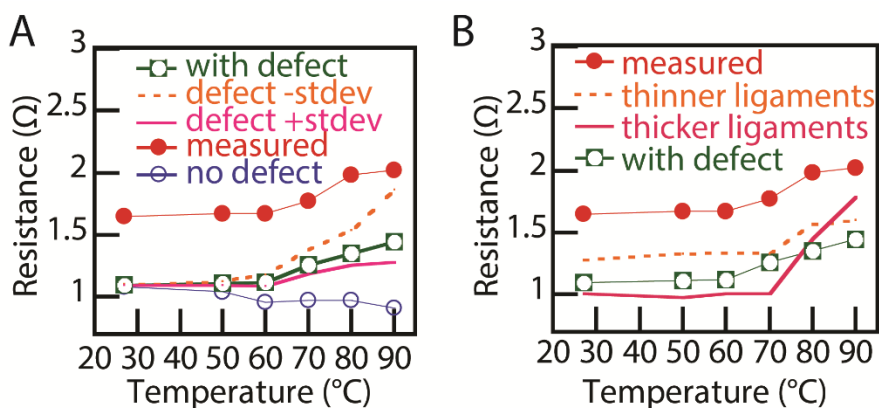


**Figure S3.** A) Resistance versus temperature for measured and simulated resistance values. Effect of varying defect spacing on resistance values is demonstrated. B) Effect of varying ligament size on resistance is demonstrated in resistance versus temperature plot. For resistance calculation with thinner ligament sizes 1<sup>st</sup> quartile cutoff (obtained from image analysis) was used for each sample. For thicker ligaments 3<sup>rd</sup> quartile was used for resistance calculations.

## References

1. T. S. Dorofeeva and E. Seker, *Nano Research*, 2015, **8**, 2188-2198.
2. Y. Ding, Y. J. Kim and J. Erlebacher, *Advanced Materials*, 2004, **16**, 1897-1900.
3. J. Wang, R. Xia, J. Zhu, Y. Ding, X. Zhang and Y. Chen, *Journal of Materials Science*, 2012, **47**, 5013-5018.